IJNAOE
©SNAK, 2015

Int. J. Nav. Archit. Ocean Eng. (2015) 7:626~639
http://dx.doi.org/10.1515/ijnaoe-2015-0044
pISSN: 2092-6782, eISSN: 2092-6790

Experimental and numerical study on ice resistance for icebreaking vessels

Jian Hu[1] and Li Zhou[2]

[1]*College of Shipbuilding Engineering, Harbin Engineering University, Harbin, China*
[2]*Aker Solutions, Fornebu, Norway*

Received 29 October 2014; Revised 11 March 2015; Accepted 30 March 2015

ABSTRACT: *Ice resistance is defined as the time average of all longitudinal forces due to ice acting on the ship. Estimation of ship's resistance in ice-covered waters is very important to both designers and shipbuilders since it is closely related to propulsion of a ship and it determines the engine power of the ship. Good ice performance requires ice resistance should be as low as possible to allow different manoeuvres. In this paper, different numerical methods are presented to calculate ice resistance, including semi-analytical method and empirical methods. A model test of an icebreaking vessel that was done in an ice basin has been introduced for going straight ahead in level ice at low speed. Then the comparison between model test results and numerical results are made. Some discussions and suggestions are presented as well to provide an insight into icebreaking vessel design at early stage.*

KEY WORDS: Ice resistance; Ice resistance formulas; Model test data; Icebreaking vessels.

INTRODUCTION

Growing interest in shipping and drilling operations in ice-covered waters has triggered more investigation on ice loads estimation. Understanding and calculating ice loads form the basis of ship design for ice. For icebreakers and icebreaking vessels, ice resistance estimation is a key mission in preliminary stage of design process and highly related to ship's global performance. Once a certain hull is determined, it is important for designers to have insight into ice loads in order to select propeller and propulsion system which meet power requirement of the ship. The hull designed is expected to undertake low ice resistance and have good performance in ice under certain ice conditions.

Many researchers has done research on ice resistance and thus developed a lot of empirical and analytical formulas since 1970. Enkvist et al. (1979) discussed the main phenomena in the level ice-breaking process. Keinonen et al. (1996) presented equations to calculate ice resistance for a ship traveling at low velocity in level ice based on massive full scale measurements on icebreakers. Riska et al. (1997) proposed a formula to calculate ice resistance. In particular, some researchers divided level ice-hull interaction process into several phases, including ice breaking, rotating, sliding and clearing (Lewis and Edwards, 1970; Kotras et al., 1983; Lindqvist, 1989; Spencer et al., 2001; Valanto, 2001; Jeong, 2010).

More recently, some researchers began to develop numerical simulation in time domain. Wang (2001) initialized a method

Corresponding author: *Li Zhou*, e-mail: *zhouli209@hotmail.com*

for simulating the interaction between moving level ice and a fixed conical structure. Based on the ice failure model derived by Wang (2001), Su et al. (2010) refined the ice-ship contact procedure to simulate ship manoeuvres in level ice. The numerical analysis was validated by comparing simulations with ship performance data of icebreaker Tor Viking II.

However, no single and exact method to calculate ice resistance exists. In this paper, a numerical method in time domain and several typical ice resistance formulas often used are described. The calculated results are compared with those from the model tests. Some discussions and suggestions on selections of formulas and how to make a reasonable prediction on ice resistance are made. This might provide help to icebreaker designers to some extent.

METHOD OF NUMERICAL SIMULATION IN TIME DOMAIN

In the present simulation, there are two reference frames used, see Fig. 1.

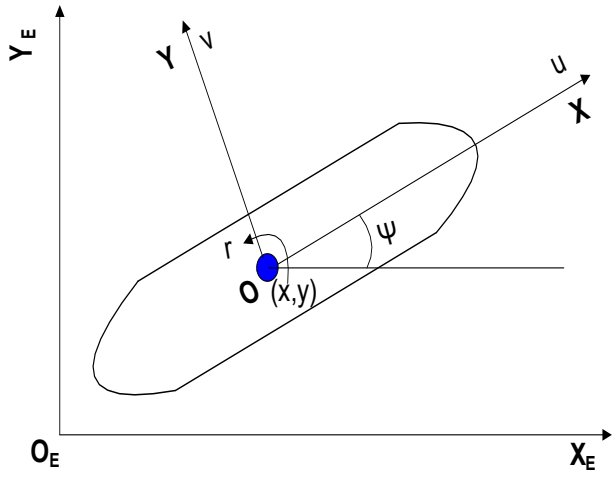

Fig. 1 Earth-fixed ($X_EY_EZ_E$) and body-fixed (XYZ) reference frames in the horizontal plane.

- The Earth-fixed frame, denoted as $X_EY_EZ_E$, is placed so that the X_EY_E plane coincides with the water surface, and the Z_E axis is positive downwards.
- The body-fixed frame, denoted as XYZ, is fixed to the vessel in such a way that the origin coincides with the centre of gravity, the X-axis is directed from aft to fore along the longitudinal axis of the hull, and the Y-axis is directed to the starboard.

The horizontal position and orientation of the vessel in the Earth-fixed coordinate system are defined by $\boldsymbol{\eta} = [x, y, \psi]$, where the first two variables describe the position and the last variable describes the heading angle. Correspondingly, the translational and rotational body-fixed velocities are defined by $\mathbf{V} = [u, v, r]$. The body-fixed general velocities are transformed to the Earth-fixed frame by

$$\dot{\boldsymbol{\eta}} = \mathbf{J}(\boldsymbol{\eta})\mathbf{v} \tag{1}$$

$$\mathbf{J}(\boldsymbol{\eta}) = \begin{bmatrix} c\psi & -s\psi & 0 \\ s\psi & c\psi & 0 \\ 0 & 0 & 1 \end{bmatrix} \tag{2}$$

where c, s are compact notations for cosine and sine, respectively.

The equation of motion is first expressed in the Earth-fixed coordinate system and then converted to the body-fixed coordinate system. Based on Newton's second law, the linear coupled differential equations of motion in the body-fixed coordinate can be written in the following form:

$$\mathbf{(M+A)\ddot{r}(t)+B\dot{r}(t)+Cr(t)=F}_e\mathbf{(t)} \tag{3}$$

$$\mathbf{F}_e(\mathbf{t})=\begin{bmatrix}R_{b1}\\R_{b2}\\R_{b6}\end{bmatrix}+\begin{bmatrix}R_{s1}\\R_{s2}\\R_{s6}\end{bmatrix}+\begin{bmatrix}R_{r1}\\R_{r2}\\R_{r6}\end{bmatrix}+\begin{bmatrix}F_{m1}\\F_{m2}\\F_{m6}\end{bmatrix}+\begin{bmatrix}F_{ow1}\\F_{ow2}\\F_{ow6}\end{bmatrix}+\begin{bmatrix}0\\0\\M_{\psi}\end{bmatrix}+\begin{bmatrix}mvr\\-mur\\0\end{bmatrix} \tag{4}$$

where $\dot{\mathbf{r}}=\mathbf{V}$, the added mass matrix A in open water is calculated from a boundary element method routine, the damping term B is assumed to be zero in the stationkeeping mode, the hydrostatic restoring coefficient C is zero. The subscripts 1, 2 and 6 refer to the directions of surge, sway, and yaw. The notation R_b is the ice-breaking force, which will be described in Section 3.1.The notation R_s is the ice submersion force,while the notation R_r denotes the ice force due to ice rubble accumulation. F_m is the restoring force due to the mooring system translated from the earth-fixed coordinate system to body-fixed coordinate system by the rotation matrix. The notation F_{ow} is the drag force due to the motion of the ship relative to the water. The notation M_Ψ represents the moment produced by the heading controller, which is zero if not used in the simulation. The last term in Eq. (4) is due to the translation from the earth-fixed coordinate system into the body-fixed coordinate system. Newmark's method is used to solve the resulting equations of motion.

The ice loads acting on a ship depends significantly on the interaction process by which the hull breaks and displaces the ice. Once the ice contacts the hull, ice is being crushed. The crushing force then increases with increasing contact area until its vertical force component gets large enough to cause bending failure of the ice, after which the broken ice floes start to turn along the ship's hull until they are parallel to the hull. Finally, the floes submerge and slide along the hull as they are pushed by the next broken ice floes. With this concept in mind, an ice force model composed of an ice-breaking model and an ice submersion model is briefly described.

Ice breaking model

The ice-breaking model introduced by Su et al. (2010), is used herein. The basic geometric model for ice–hull interaction includes the full-size waterline of the ship and the edge of the ice. As shown in Fig. 2, the waterline of the ship is discretized into a closed polygon and the edge of the ice is discretized into a poly line in the established simulation program. At each time step, the simulation program is set to detect the ice nodes which are inside the hull polygon. Then, each contact zone can be found. To check whether the ice node is inside the hull polygon, geometric tools from computer graphics are adopted. It is assumed that the contact surface between ice and hull is flat, and the contact area is simply determined by contact length and indentation depth. The contact length is calculated from the distance between adjacent hull nodes, and the indentation depth is calculated from the perpendicular distance from the cusp of ice nodes to the contact surface. More details are referred to Su et al. (2010).

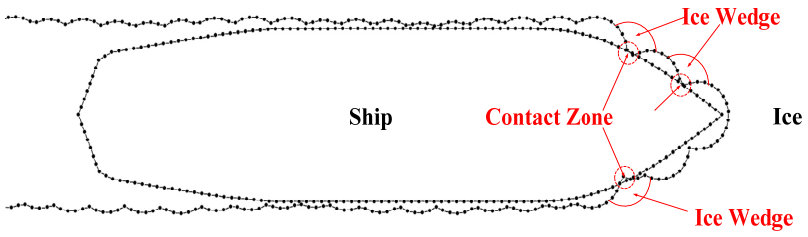

Fig. 2 Discretization of the ship hull and the edge of the ice.

The ice wedges formed in the ice breaking process were determined by bending cracks, which were idealized and described by a very important parameter, namely the icebreaking radius. The icebreaking radius R was derived from the expression given in Wang (2001):

$$R=C_l l(1.0+C_v v^{rel} n) \tag{5}$$

where v_n^{rel} is the relative normal velocity between the ice and the hull node, C_l and C_v are two empirical parameters, C_l having a positive value and C_v is a negative value, l is the characteristic length of the ice:

$$l = \left(\frac{Eh_i^3}{12(1-v^2)\rho_w g} \right)^{1/4} \tag{6}$$

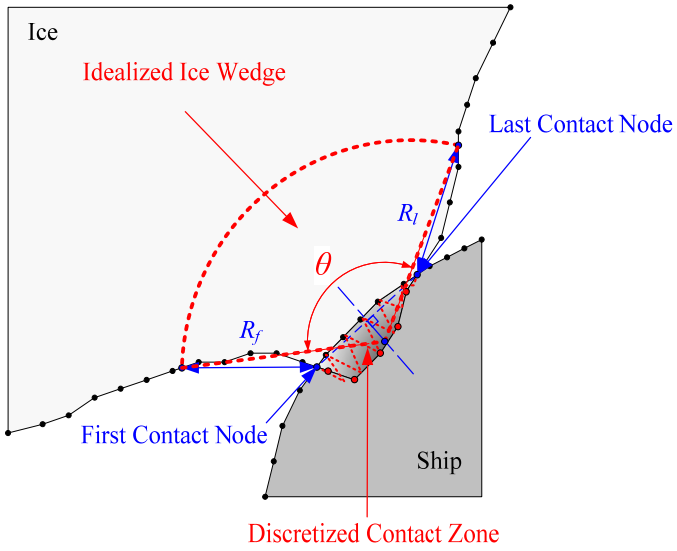

Fig. 3 Idealized ice wedge and discretized contact zone.

Fig. 3 shows that the ice wedge is determined by the interpolation of the icebreaking radius at the first and last contact nodes (i.e., R_f and R_l). The opening angle of the ice wedge is denoted as θ. In order to calculate the contact area A_c, the contact zone was discretized by a number of triangles (the triangles in Fig. 3) based on the hull nodes that were in contact with ice sheet. Then A_c can be approximated by the sum of area of the triangles.

As mentioned above, in the first phase of contact only crushing takes place on the contact surface. The resultant crushing force F_{cr} is normal to the contact surface and is calculated as the product of the effective crushing strength σ_c and the contact area A_c, where the ice pressure on the contact surface is assumed to be uniform and equal to the effective crushing strength.

The frictional force is also taken into account in this model by using a coefficient of friction. When the vertical component of the crushing and frictional forces F_V exceeds the bending failure load P_f given in Eq. (7), the ice wedge will be formed by a bending crack and break off from the edge of the ice:

$$P_f = C_f \left(\frac{\theta}{\pi}\right)^2 \sigma_f h_i^2 \tag{7}$$

where θ is the opening angle of the idealized ice wedge shown in Fig. 3, σ_f is the flexural strength of the ice, h_i is the ice thickness, and C_f is an empirical parameter.

Ice submersion model

When an ice wedge is formed and broken from intact ice sheet, it will submerge and slide down the surface of the hull. In this case, ice submersion loads introduced during the process has to be included. In this paper, the method by Croasdale (1980) is used. It is assumed that broken ice floe from intact ice sheet is continuously cleared around the structure by some other mechanism and doesn't contribute to ice pile up in front of the structure. The interaction between an ice sheet and a structure sloping at angle α from the horizon is shown in Fig. 4.

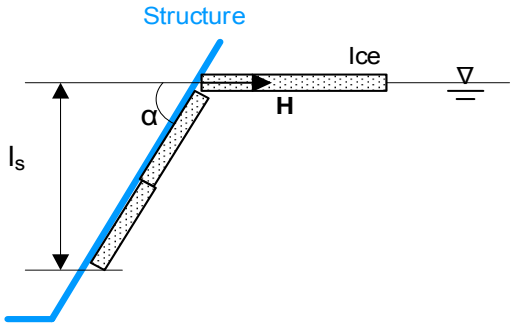

Fig. 4 Geometry for two-dimensional analysis of forces on a sloping structure.

Then the horizontal ice force arouse during ice rotation and sliding process on the sloped hull element per unit width H is written as

$$H = l_s \delta \rho h_i g(\sin\alpha + \mu\cos\alpha)(\frac{\sin\alpha + \mu\cos\alpha}{\cos\alpha - \mu\sin\alpha} + \frac{\cos\alpha}{\sin\alpha}) \tag{8}$$

where l_s is the vertical distance that ice is pushed down the slope, $\delta\rho$ is the density difference between water and ice, h_i is the ice thickness, g is the acceleration of gravity, μ is the friction coefficient between ice and the structure.

EMPIRICAL AND ANALYTICAL FORMULAS

As mentioned above, there are many empirical and analytical formulas available to estimate ice resistance. Some of them are presented as follows.

Lindqvist formula

The Lindqvist formula was developed from research done on full scale tests in the Bay of Bothnia (Lindqvist, 1989). It is a rather simple way of estimating the ice resistance. In this model, the resistance is divided into crushing, bending-induced breaking and submergence. The formula gives resistance as a function of main dimensions, hull form, ice thickness, ice friction and strength. The formula is expressed as:

$$R_{ice} = (R_c + R_b)(1 + 1.4\frac{V}{\sqrt{gh_i}}) + R_s(1 + 9.4\frac{V}{\sqrt{gL}})$$

$$R_c = 0.5\sigma_b h_i^2 \frac{\tan\phi + \mu\cos\phi/\cos\psi}{1 - \mu\sin\phi/\cos\psi}$$

$$R_b = \frac{27}{64}\sigma_b B \frac{h_i^{1.5}}{\sqrt{\frac{E}{12(1-\nu^2)g\rho_w}}} \frac{\tan\psi + \mu\cos\phi}{\cos\psi\sin\alpha}(1 + \frac{1}{\cos\psi}) \tag{9}$$

$$R_s = (\rho_w - \rho_i)gh_i B(T\frac{B+T}{B+2T} + k)$$

$$k = \mu(0.7L - \frac{T}{\tan\phi} - \frac{B}{4\tan\alpha} + T\cos\phi\cos\psi\sqrt{\frac{1}{\sin\phi^2} + \frac{1}{\tan\alpha^2}})$$

$$\psi = \arctan(\frac{\tan\phi}{\sin\alpha})$$

where R_{ice}, R_c and R_b and R_s are total andice resistance, crushing resistance, bending resistance and resistance due to submersion; σ_b and h_i are respectively ice strength in bending and ice thickness; μ, ϕ, α and ψ are respectively the friction coefficient, stem angle, waterline entrance angle and flare angle; g is the gravity acceleration; ρ_w *and* ρ_i are water and ice density; E, and υ are Young's modulus and Poisson ratio of sea ice respectively. B, T, and L are ship's breadth, draught and waterline length; V is ship speed.

Keinonen formulas

Based on results of a study of escort operations involving five icebreaking vessels, Keinonen et al. (1996) did research on resistance of icebreaking vessels in level ice. In order to investigate low-velocity ice resistance, specific formulas were derived from full scale trials of icebreaker performance in ice at 1 *m/s* speeds. These prediction formulas include parametric influences for different vessel dimensions, hull forms, hull surface conditions, ice strengths and ambient temperatures. The resistance formula is written as:

$$R = 0.08 + 0.017 C_s C_h B^{0.7} L^{0.2} T^{0.1} H^{1.25} k_1 k_2$$

$$k_1 = (1 - 0.0083(t + 30))(0.63 + 0.00074\sigma_f) \tag{10}$$

$$k_2 = (1 + 0.0018(90 - \psi)^{1.4})(1 + 0.04(\varphi - 5)^{1.5})$$

where R is total ice resistance in MN; C_s is water salinity coefficient (0 fresh, 1 saline); C_h is hull condition coefficient (1 inerta, 1.33 bare steel); B, T and L are ship beam at waterline, draft and waterline length in meter ; ψ and φ are average flare angle and buttock angle in degree; t is air temperature; σ_f is flexural strength; H is ice thickness.

Riska formulas

Riska et al. (1997) proposed a level ice resistance formula by modifying the formulations of Lindqvist (1989). The formulation is based on a set of empirical coefficients, derived from full- scale tests of a number of ships in ice conditions in the Baltic Sea. The main resistance formula is given in Eq. (11), while constants are found in Table 1.

$$R_{ice} = C_1 + C_2 V$$

$$C_1 = f_1 \frac{1}{\frac{2T}{B} + 1} BL_{par} h_i + (1 + 0.021\phi)(f_2 B h_i^2 + f_3 L_{bow} h_i^2 + f_4 B L_{bow} h_i) \tag{11}$$

$$C_2 = (1 + 0.063\phi)(g_1 h_i^{1.5} + g_2 B h_i) + g_3 h_i (1 + 1.2T / B) \frac{B^2}{\sqrt{L}}$$

where V, B, T and L are vessel speed, breadth, draught and length, h_i is ice thickness, ϕ is the stem angle in degrees and L_{bow} and L_{par} are the length of bow and parallel sides section, respectively.

Table 1 Constants in Riska formulation for ice resistance in level ice.

Symbol	Value	Unit
f_1	0.23	$[kN/m^3]$
f_2	4.58	$[kN/m^3]$
f_3	1.47	$[kN/m^3]$
f_4	0.29	$[kN/m^3]$
g_1	18.9	$[kN/(m/s*m^{1.5})]$
g_2	0.67	$[kN/(m/s*m)]$
g_3	1.55	$[kN/(m/s*m^{2.5})]$

Jeong formulas

Jeong (2010) proposed new ice resistance prediction formula for standard icebreaker model using component method of ice resistance and also predicted the model test results to full-scale using calculated non-dimensional coefficients. The formulas are presented as follow:

$$R_I = 13.14V^2 + C_B \Delta \rho g h_i BT + C_c F_h^{-\alpha} \rho_i B h_i V^2 + C_{BR} S_N^{-\beta} \rho_i B h_i V^2$$

$$F_h = \frac{V}{\sqrt{g h_i}} \tag{12}$$

$$S_N = \frac{V}{\sqrt{\frac{\sigma_f h_i}{\rho_i B}}}$$

where R_I total ice resistance; C_B, C_C and C_{BR} are coefficient of ice buoyancy resistance, coefficient of ice clearing resistance and coefficient of ice breaking resistance; F_h and S_N are Froude number and strength number; α is index of Froude number; β is index of Strength number; ρ_i and ρ_w are ice and water density; $\Delta\rho$ is water density minus ice density; g is gravitational constant; h_i is ice thickness; B and T are beam and draft of the ship; V is ship speed; σ_f = flexural strength of ice. The constants used are shown in Table 2.

Table 2 Constants in Jeong formulation for ice resistance in level ice.

Symbol	Value
C_B	0.5
C_C	1.11
C_{BR}	2.73
α	1.157
β	1.54

Model test description

Zhou et al. (2013) carried out a series of model tests in the ice basin of the Marine Technology Group in the Aalto University, where the icebreaking tanker MT Uikku was deployed. A scaling factor of λ=31.56 was used for all tests. The

model was trimmed to even keel without heel angle, so that the center of buoyancy and the center of gravity were in the same longitudinal and transverse location. The particulars of the model and full scale vessel are given in Table 3.

Table 3 Full-scale primary dimensions of MT Uikku.

Item	Notation	Unit	Value
Length	L	*m*	150.0
Length of bow	L_{bow}	*m*	39
Length of parallel	L_{par}	*m*	65
Breadth moulded	B	*m*	21.3
Tested draft	T	*m*	9.5
Bow waterline angle	α	*deg*	21
Bow stem angle	ϕ	*deg*	30
average flare angle	ψ	*deg*	58

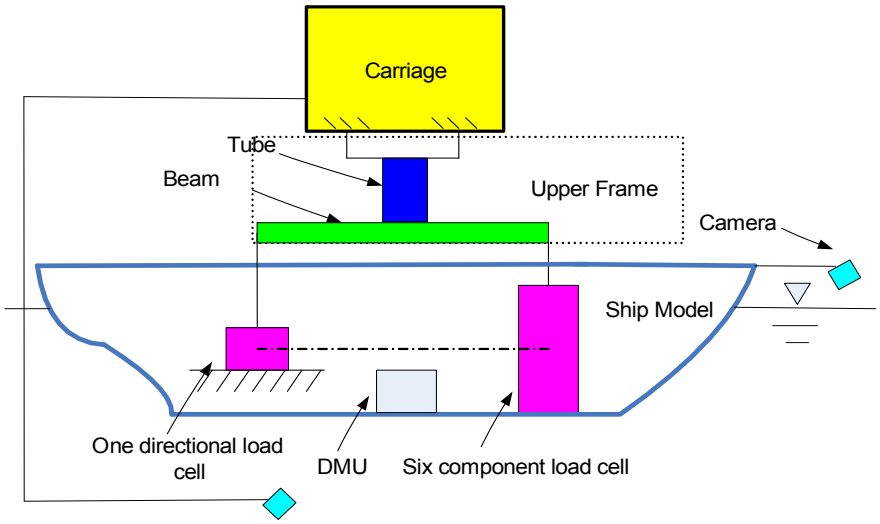

Fig. 5 Side view illustration shoeing the components of the test system.

The instrumentations, including a compact 6-component force transducer, one-directional load cell, a dynamic measurement unit and two cameras, were installed to the ship model. The configuration is shown in Fig. 5. The ship model was constrained so that the six force components could be measured. An upper frame with a stiff tube and long beam was used to connect the towing carriage with the load measurement units rigidly, which were attached to the ship model. The measurement data was sampled at a rate of 107 *Hz*.

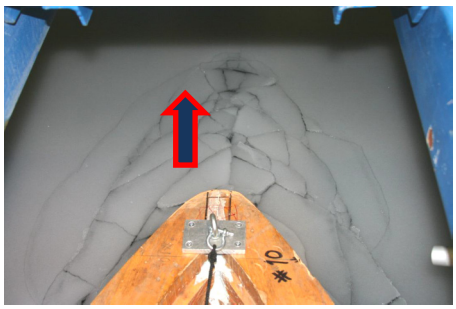

Fig. 6 Icebreaking at bow (Zhou et al., 2013).

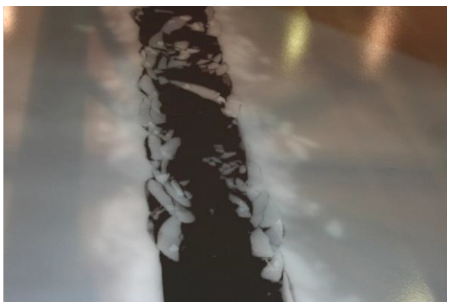

Fig. 7 Open channel after test (Zhou et al., 2013).

As shown in Fig. 6, the ship model was towed straight against unbroken ice at constant predefined speeds by the carriage above the ship model. The open channel created by travelling of the ship model is shown in Fig. 7. Test matrix and measured ice properties are presented in Table 4.

Table 4 Test matrix with head on cases and measured ice properties.

Ice sheet	Test No.	h_i [*m*]	σ_b [*kPa*]	σ_c [*kPa*]	E_i [*MPa*]	V_i [*m/s*]	ψ [*deg*]
I	103	0.77	724	1748	929	0.2	0
	104	0.76	844	2192	984	0.5	0
II	205	0.96	920	1840	1685	0.2	0
	206	0.95	912	1862	1701	0.5	0

COMPARISONS AND DISCUSSIONS

Time domain simulations are performed in order to compare model test results. In addition, ice resistances by empirical and analytical formulas are calculated and compared with model test results. Some parameters could be derived from Tables 1-4. The other parameters used in the calculation are shown in Table 5.

Table 5 The other parameters in the calculation.

Items	Unit	Value
Poisson's ratio ν	-	0.33
Ice-hull friction coefficient μ	-	0.04
Water density ρ_w	kg/m^3	989
Ice density ρ_i	kg/m^3	906
C_s	-	1.0
C_h	-	1.0
C_B	-	0.5
C_C	-	1.11
C_{BR}	-	2.73

Numerical simulation and model test results

Typical time histories of ice forces in the longitudinal direction for all head-on tests from both model test and numerical simulation are presented in Fig. 8. The presented time signals are filtered with an extreme low cut-off frequency in order to show the general evolution of ice forces in time domain. A comparison of results in a quantitative way is made, where the mean values, standard deviations and steady value of the ice forces at the end stage of model test are presented. The differences between simulated data and model test data are explained and identified to some extent.

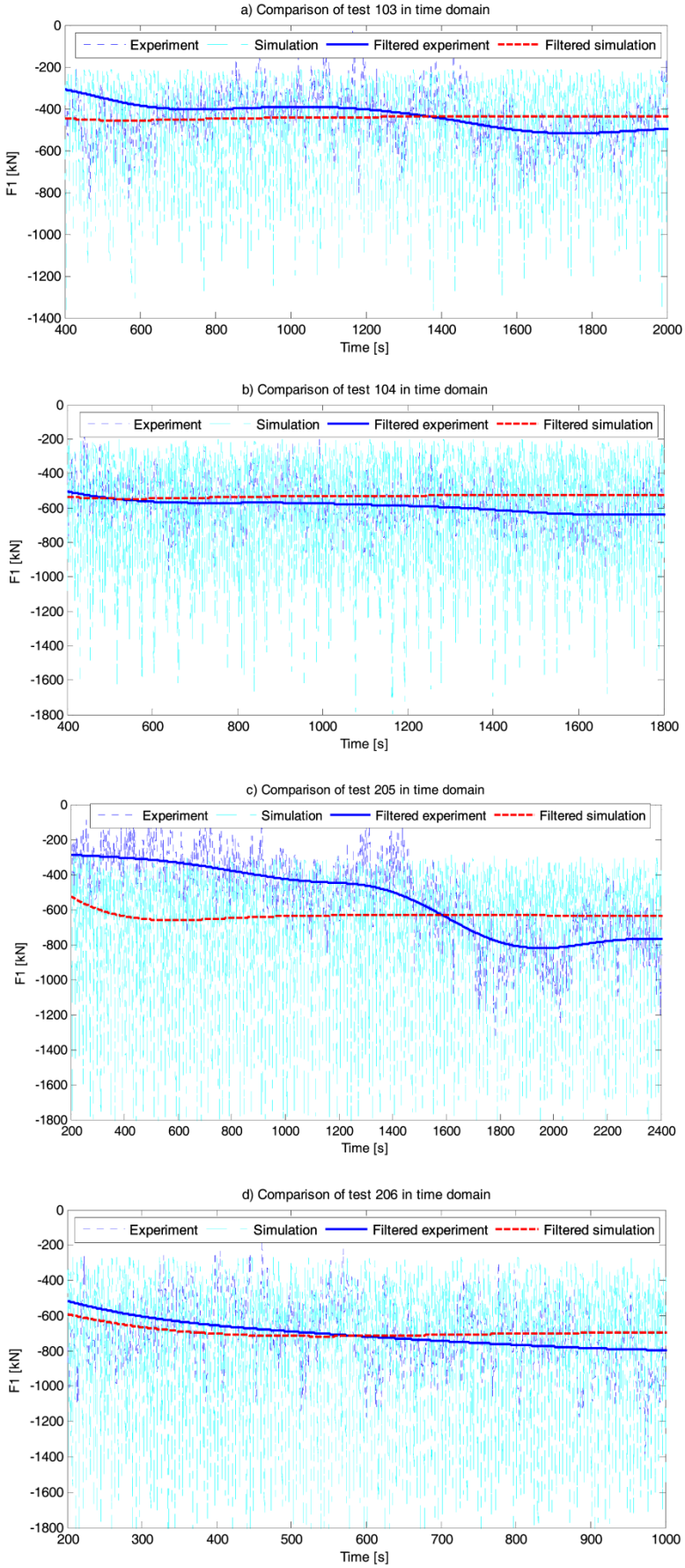

Fig. 8 Comparisons between numerical simulation and model test in time domain.

Table 6 Experimental and simulated level ice forces for zero heading cases.

Test No.	Model test (*kN*)			Numerical simulation (*kN*)		
	Mean	Std.	Steady	Mean	Std.	Steady
103	470	120	500	440	190	440
104	560	120	640	530	230	530
205	670	220	770	630	290	640
206	720	200	800	690	320	700

From Fig. 8, it is clear that the numerical simulations capture main trend that was obtained from model test. The smoothed ice forces from simulation approaches to the measured force from the experiment. From Table 6, it is seen that a good agreement is achieved for the mean values of ice forces in the longitudinal direction (ice resistance).

The simulated standard deviation and peak forces are a little higher than the measured value. This is attributed to inherent limitation of the numerical model. In the present numerical model, it is assumed that the broken ice is cleared away immediately after it is broken away from the intact level ice. This is not the case in reality. The broken ice cusp will rotate against the hull, especially at shoulder area to the mid-hull area. After the cusp is broken away from the intact ice, it might be crushed by the hull side in the rotation process until the cusp is parallel to the hull side, which brings in a large transverse force. This phenomenon is hard to reproduce since this process is random in nature. It is very difficult to predict exactly when and where the crushing of broken cusp occurs.

In addition, there exist some deviations between the simulated and measured forces at the steady stage (see Table 6). It should be noted that simulated ice resistances in steady stage almost keep constant while the resistances are increasing for all cases in the model test. The simulated steady ice forces are 15% lower approximately. The main reason is that the broken ice floes accumulated around the hull steadily in the model test, but the ice force calculated due to broken ice floes is assumed to be constant when using the present numerical model. As time goes, more and more broken ice floes may submerge, slide and accumulate at the bow area and even go under the bottom of the hull. However, this mechanism is not considered in the present numerical model.

Empirical and model test results

The empirically calculated results and model test measurements are shown in Table 7. The corresponding results are plotted in Fig. 9 for comparison.

Comparing ice resistance by Lindqvist formulas and model test, it is found the Lindqvist formulas give the lowest prediction among these methods. The highest deviation is around 50% for test 103. The Lindqvist formulas were well evaluated against full scale tests with different ships, but the comparison was done with ice thickness less than 0.65 *m*. It might be not applicable to estimate level ice resistance of ship in thick ice (>0.65 *m*), as used in the model test. Lindqvist formulas were evaluated against full scale measurements of several icebreakers in the Baltic, where the ice conditions are identical. How changes in mechanical properties of the ice affect the resistance is still the greatest uncertainty to use the formulas. The full scale tests were done in ice with bending strength up to 660 *kPa*, but this value has increased to 920 *kpa* in the model test 205. The ship model might need much more energy to break ice. Lindqvist formulas do not take the effect of crushing strength into account. This might be reasonable for ice in the Baltic with low crushing strength, but the crushing force could be under estimate when high crushing are very large in the model test. The resistance dependency on vessel speed seems to be reasonable.

The ice resistance calculated with Riska formulas is slightly higher (17%~30%) than the model test results. Similar to Lindqvist formula, the Riska formulation assumes a linear relationship between vessel speed and ice thickness. An important difference is however that Riska does not normalize the velocity, which may influence the result to some degree.

Ice thickness, flexural strength and friction coefficient are important factors in prediction of total ice resistance by Jeong's theoretical method. Only one case was predicted well. They seem to be sensitive to vessel speed, which might bring some trouble to ice resistance estimation. Ice buoyancy resistance is calculated from pre-sawn ice test with creeping speed test. The dimensionless ice buoyancy resistance coefficient, C_B was found to be 0.50 for friction coefficient μ=0.02 according to Jeong (2010). However, this parameter is 0.04 in the model tests. It is unclear that how the friction coefficient affects the buoyancy resistance coefficient.

Table 7 Experimental and simulated level ice forces for head-on cases (in *kN*).

Case No.	Model test	Numerical simulation	Empirical and analytical formulas					
			Lindqvist	Riska	Jeong	Keinonen[1]	Keinonen[2]	Average
1 (Test 103)	470	440	320	610	330	650	510	440
2 (Test 104)	560	530	380	630	520	690	600	530
3 (Test 205)	670	630	510	800	560	930	740	650
4 (Test 206)	720	690	560	840	800	920	810	750

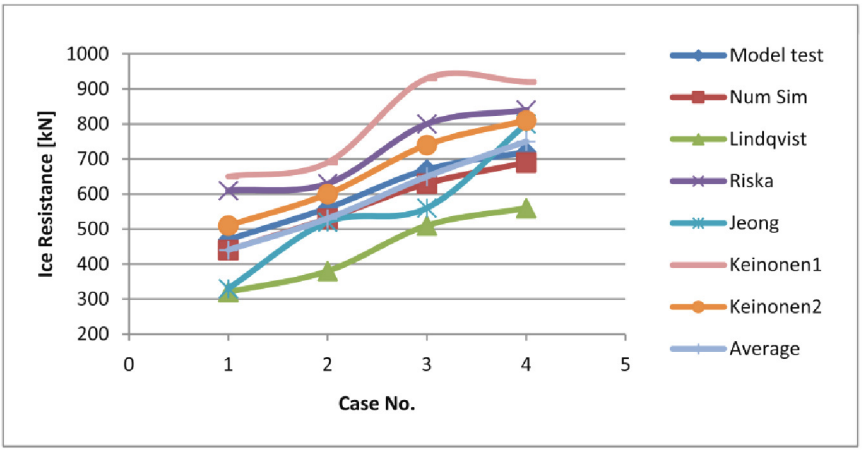

Fig. 9 Comparison of experimental and simulated ice resistance.

It should be noted that the lowest vessel speed for using Keinonen formula is 1 *m/s*. The calculated results at this speed are shown in Table 7, noted by Keinonen[1]. Apparently, it is very conservative compared to model test results. But in the model tests, all vessel speeds are below 1 *m/s*. Correction must be made to consider the effect of vessel speeds at the range below 1 *m/s*. Herein, this effect presented in Lindqvist formulas is suggested. The ice crushing and breaking forces are dominant. So the correction factor C_f is a function of vessel speed, ice thickness and gravity acceleration, which is express as (V_1= 1 *m/s*):

$$C_f = \frac{1+\frac{V}{\sqrt{gh_i}}}{1+\frac{V_1}{\sqrt{gh_i}}} \tag{13}$$

The corrected ice resistance is equal to the ice resistance at 1 *m/s* with Keinonen formula multiplied by correction factor. The correction factors for each case are shown in Table 8. Corrected ice resistances Keinonen[2] are lower than those uncorrected, but still over measured ice resistance.

Table 8 Correction factors for Keinonen formula.

Case No.	Correction factor
1 (Test103)	0.78
2 (Test104)	0.87
3 (Test 205)	0.80
4 (Test 206)	0.88

Based on comparisons made above, it is found that every empirical and analytical method has its own advantages and disadvantages. Care should be taken when designers use these formulas. The conditions under which the formulas are suitable should be well evaluated before using them. Under the condition of unknown ice conditions, a general suggestion is to use all those formulas to do a comprehensive analysis to balance pros and cons inherently in those formulas. As shown in Table 7, ice resistances calculated by all empirical formulas described in the paper (except Keinonen[1]) are averaged. The averaged value agrees well with measured ones (See Fig. 9).

CONCLUSIONS

This paper aims to study ice resistance in both numerical and experimental ways. A numerical simulation method and some empirical and analytical methods to calculate ice resistance are presented in details. The calculated results are compared against model test results.

All empirical methods mentioned in the present paper could predict ice resistance at different accuracy, but any of them could give a good estimation for all cases. A more practical suggestion is to use all empirical formulas and calculate the average value. However, they could be only used in the conceptual design phase and cannot take the details of hull lines into consideration. The numerical simulation method is a relatively complex method considering the bow shape, but could provide reasonable prediction of ice resistance in time domain.

ACKNOWLEDGEMENTS

Project supported by the National Natural Science Foundation of China (Grant Nos. 11102048, 11302057) and the Specialized Research Fund for the Doctoral Program of Higher Education of China (Grant No. 20132304120028) .

REFERENCES

Croasdale, K.R., 1980. *Ice forces on fixed, rigid structures. In: CRREL special report 80-26, working group on ice forces on structures*. *a state-of-the-art report*. Hanover: U.S. Army.

Enkvist, E., Varsta, P. and Riska, K., 1979. *The ship-ice interaction. Proceedings of the 5th International Conference on Port and Ocean Engineering under Arctic Conditions, Trondheim, Norway, 13-17 August 1979*. pp.977-1002.

Jeong, S.Y., Lee, C.J. and Cho, S.R., 2010. Ice Resistance Prediction for Standard Icebreaker Model Ship. *Proceedings of the Twentieth (2010) International Offshore and Polar Engineering Conference, Beijing, China, 20-25 June 2010.* pp. 1300-1304.

Keinonen, A.J., Browne, R., Revill, C. and Reynolds, A., 1996. *Icebreaker characteristics synthesis, report TP 12812E*. Ontario: The Transportation Development Centre, Transport Canada.

Kotras, T.V., Baird, A.V. and Naegle, J.N., 1983. Predicting ship performance in level ice. *Transactions of Society of Naval Architects and Marine Engineers (SNAME)*, 91, pp.329-349.

Lewis, J.W. and Edward, Y., 1970. Methods for predicting icebreaking and ice resistance characteristics of icebreakers. *SNAME Transactions*, 78, pp.213-249.

Lindqvist, G., 1989. A straightforward method for calculation of ice resistance of ships. *Proceedings of 10th International Conference on Port and Ocean Engineering under Arctic Conditions (POAC)*, Lulea, Sweden, 12-16 June 1989, pp. 722-735.

Riska, K., Wilhelmson, M., Englund, K. and Leiviskä, T., 1997. *Performance of merchant vessels in the baltic. Research report no 52*. Espoo: Helsinki university of technology, ship laboratory, Winter Navigation Research Board.

Spencer, D. and Jones, S.J., 2001. Model-scale/full-scale correlation in open water and ice for canadian coast guard "R-Class" icebreakers. *Journal of Ship Research*, 45(4), pp.249-261.

Su, B., Riska, K. and Moan, T., 2010. A numerical method for the prediction of ship performance in level ice. *Cold Regions Science and Technology*, 60(3), pp.177-188.

Valanto, P., 2001. The resistance of ships in level ice. *SNAME Transactions*, 109, pp.53-83.

Wang, S., 2001. *A dynamic model for breaking pattern of level ice by conical structures*. Ph.D. Thesis. Department of Mechanical Engineering, Helsinki University of Technology, Finland.

Zhou, L., Riska, K., von Bock, P., R., Moan, T. and Su, B., 2013. Experiments on level ice loading on an icebreaking tanker with different ice drift angles. *Cold Regions Science and Technology*, 85, pp.79-93.